Predictive nomogram using multimodal ultrasonographic features for axillary lymph node metastasis in early-stage invasive breast cancer

JIEJIE YAO[1*], WEI ZHOU[1*], YING ZHU[1], JIANQIAO ZHOU[1], XIAOSONG CHEN[2] and WEIWEI ZHAN[1]

[1]Department of Ultrasound; [2]Comprehensive Breast Health Center, Ruijin Hospital, School of Medicine, Shanghai Jiao Tong University, Shanghai 200025, P.R. China

Received August 10, 2023; Accepted December 19, 2023

DOI: 10.3892/ol.2024.14228

Abstract. Axillary lymph node (ALN) status is a key prognostic factor in patients with early-stage invasive breast cancer (IBC). The present study aimed to develop and validate a nomogram based on multimodal ultrasonographic (MMUS) features for early prediction of axillary lymph node metastasis (ALNM). A total of 342 patients with early-stage IBC (240 in the training cohort and 102 in the validation cohort) who underwent preoperative conventional ultrasound (US), strain elastography, shear wave elastography and contrast-enhanced US examination were included between August 2021 and March 2022. Pathological ALN status was used as the reference standard. The clinicopathological factors and MMUS features were analyzed with uni- and multivariate logistic regression to construct a clinicopathological and conventional US model and a MMUS-based nomogram. The MMUS nomogram was validated with respect to discrimination, calibration, reclassification and clinical usefulness. US features of tumor size, echogenicity, stiff rim sign, perfusion defect, radial vessel and US Breast Imaging Reporting and Data System category 5 were independent risk predictors for ALNM. MMUS nomogram based on these factors demonstrated an improved calibration and favorable performance [area under the receiver operator characteristic curve (AUC), 0.927 and 0.922 in the training and validation cohorts, respectively] compared with the clinicopathological model (AUC, 0.681 and 0.670, respectively), US-depicted ALN status (AUC, 0.710 and 0.716, respectively) and the conventional US model (AUC, 0.867 and 0.894, respectively). MMUS nomogram improved the reclassification ability of the conventional US model for ALNM prediction (net reclassification improvement, 0.296 and 0.288 in the training and validation cohorts, respectively; both P<0.001). Taken together, the findings of the present study suggested that the MMUS nomogram may be a promising, non-invasive and reliable approach for predicting ALNM.

Introduction

Breast cancer (BC) is the most commonly diagnosed cancer worldwide, with an estimated 2.3 million new cases (11.7%) and has ranked the fifth leading cause (6.9%) of cancer death (1). Axillary lymph node (ALN) status is a key prognostic factor for patients with early-stage invasive BC and influences the clinical therapeutic schedule. The guidelines of the American Society of Clinical Oncology and the Z0011 trial have demonstrated that patients with early-stage BC with <2 sentinel lymph node (SLN) metastases can be spared ALN dissection (ALND) (2,3). SLN biopsy is still the current standard approach for the assessment of ALN status. However, it has been criticized for its low efficiency and invasive complications, including upper arm numbness, lymphedema, nerve damage and hematoma (4,5). Therefore, developing an accurate and non-invasive method to predict ALN status before surgery remains a challenge.

Ultrasound (US) has potential clinical benefits for performing breast examinations due to low cost, convenience and lack of radiation. Axillary US examination is a simple and convenient diagnostic method to detect ALNM but its value is limited due to its low sensitivity (26.4-69.5%), especially for patients with a minor ALN metastatic burden (6). US-guided fine needle aspiration is an invasive procedure and its high accuracy is influenced by the inadequate sample collection (7).

Correspondence to: Professor Weiwei Zhan, Department of Ultrasound, Ruijin Hospital, School of Medicine, Shanghai Jiao Tong University, 197 2nd Ruijin Road, Shanghai 200025, P.R. China
E-mail: shanghairuijinus@163.com

*Contributed equally

Abbreviations: ALNM, axillary lymph node metastasis; AUC, area under the curve; BI-RADS, Breast Imaging and Reporting Data System; CEUS, contrast-enhanced ultrasound; DCA, decision curve analysis; ER, estrogen receptor; HER2, human epidermal growth factor receptor 2; IBC, invasive breast cancer; MM, multimodal; NRI, net reclassification improvement; PR, progesterone receptor; ROC, receiver operating characteristic; SE, strain elastography; SLN, sentinel lymph node; SWE, shear wave elastography

Key words: predictive nomogram, multimodal ultrasound, early-stage breast cancer, axillary lymph node metastasis

'Radiomics' has attracted increased attention in (8-10). Several studies (8-10) have predicted the likelihood of ALNM based on US radiomics. However, certain radiomics analyses are limited by single-modal grayscale US images, and the values of the area under the receiver operator characteristic (ROC) curve (AUC) were found to be relatively low (0.71-0.73) (8,9). A recent study reported construction of a shear wave elastography (SWE) US-based radiomics nomogram that yielded a moderate predictive ability, with a C-index of 0.817 (10). However, the most significant SWE radiomics features only reflected the intratumoral heterogeneity of the tumor. This does not embody the value of SWE sufficiently as SWE is known for its ability to show both intrinsic and peritumoral characteristics of the tumor via qualitative and quantitative stiffness parameters (11-13). Huang *et al* (14) designed a multimodal US (MMUS)-based auto-weighting framework for breast cancer classification. However, the MMUS analysis only involved B-mode, Doppler, strain elastography (SE) and SWE US and there was lack of valuable contrast-enhanced (CEUS) data and may be not entirely comprehensive. In addition, MMUS analysis was only used to classify BC, not to predict ALNM, and therefore was insufficient to guide clinical strategy. Other researchers have proposed deep learning radiomics models and reported favorable predictive efficacy (15,16). However, the 'black box' pattern and specialized algorithms of deep learning are hard to reproduce (14-16). Moreover, radiomics features, such as texture or wavelet, are both obscure and complex for clinicians to understand. Finally, the extraction procedures are not easy to apply in clinical practice (14,16). The aim of the present study was to establish and assess a comprehensive, concise and easy-to-use predictive tool using the combined conventional US, SE, SWE and CEUS features for preoperative ALNM risk estimation in early-stage IBC.

Materials and methods

Study design and patients. The present study was a retrospective sub-analysis of data acquired from a prospective study (17). It was conducted in accordance with the Declaration of Helsinki and approved by the Ethics Committee of Ruijin Hospital, School of Medicine, Shanghai Jiao Tong University (Shanghai, China). Written informed consent was obtained from patients. From August 2021 to March 2022, 2,003 patients with breast lesions in the Comprehensive Breast Health Center at Ruijin Hospital underwent preoperative conventional US, SE, SWE and/or CEUS examination. Conventional US + elastography was the first-line breast US examination protocol for all patients. For patients with a suspected breast tumor, CEUS examination was performed for more accurate differential diagnosis, to assess the extent of the tumor or to select necessary tumor regions for biopsy. A total of 456 patients was enrolled. The inclusion criteria were as follows: i) Diagnosis of primary early-stage IBC (stage I-II); ii) performance of breast surgery and SLN biopsy or ALND and iii) presence of preoperative multimodal US images of breast tumors and conventional US images of ALN. The exclusion criteria were as follows: i) Lack of CEUS or SE or SWE US images; ii) preoperative anticancer (neoadjuvant therapy or chemotherapy) or intervention therapy (biopsy or ablation) prior to US examination; iii) diagnosis of bilateral, multicentric or multifocal IBC; iv) presence of diffusive lesions and v) insufficient US image quality or incomplete clinicopathological data.

A total of 342 patients (all female; mean age, 51.15±11.62 years; range, 32-88 years) passed the quality control for final analysis and were randomly divided (7:3) into a training (n=240) and validation cohort (n=102), according to the Transparent Reporting of a multivariable prediction model for Individual Prognosis or Diagnosis reporting guideline (18). Fig. 1 shows the recruitment of patients and the study design.

Clinical and pathological data. Data were obtained from the medical records. The clinical data included patient age, symptoms, family history of BC, history of hormone therapy and clinical tumor stage. Pathological data included histological type, tumor grade, estrogen receptor (ER), progesterone receptor (PR), human epidermal growth factor receptor 2 (HER2) status, tumor proliferation rate (Ki67 levels) and ALN status (positive or negative). All pathological macrometastases, micrometastases or isolated tumor cells of ALNs were defined as node-positive. A cut-off value for $Ki67^+$ was established at 20% (19). Molecular subtypes were classified as luminal A or B, $HER2^+$ and triple-negative BC, according to the expression of ER, PR and HER2 (20).

US image acquisition and US-depicted ALN status. All preoperative breast and axillary US examinations were performed by two experienced radiologists (JJY and YZ) with >15 combined years of experience in breast US and 8 combined years of experience in performing SE, SWE and CEUS of breast lesions, using a 3-11 MHz linear probe (Resona 8, Shenzhen Mindray Bio-Medical Electronics Co., Ltd.). The conventional US variables, such as tumor shape, margin, orientation, echogenicity, posterior acoustic pattern, calcification and vascularity status, were assessed according to the Breast Imaging Reporting and Data System (BI-RADS) (21). The maximum size of the breast tumor, measured by US, and the US BI-RADS category were also assessed. The lymph node was depicted as positive if it had ≥1 of the following suspicious US characteristics: Circular shape, cortical thickening, calcification or cystic change, no fatty hilum or no hilar blood flow (22,23). SE features were classified as soft or hard as described previously (24). The stiff rim sign in SWE was reported as absent or present according to Zhou *et al* (25). The maximum (E_{max}), mean (E_{mean}) and minimum (E_{min}) elastic modulus and elastic modulus standard deviation (E_{SD}), calculated automatically by the US system, were recorded. CEUS examinations were performed according to the American Institute of Ultrasound in Medicine practice guidelines for performing breast CEUS (26). Contrast agent SonoVue® (Bracco S.p.A.) was reconstituted by addition of 5 ml sterile normal saline and 25 mg lyophilized powder. Following hand agitation, 2.4 ml contrast agent was injected through a 21-G catheter via a peripheral vein in a bolus fashion, followed by a flush of 5 ml saline solution. The entire CEUS process for each patient was recorded immediately following injection of the contrast agent and lasted for 180 sec. US images and video clips were stored on the hard disk for subsequent analysis. The qualitative features assessed included degree of enhancement (hypo/isoenhancement or hyperenhancement), perfusion defect (absent or present) and radial vessel at the tumor margin (absent or present). Quantitative parameters, including arrival time (AT; the time point when the microbubble arrived at the lesion), time to peak (TTP; time point when the contrast

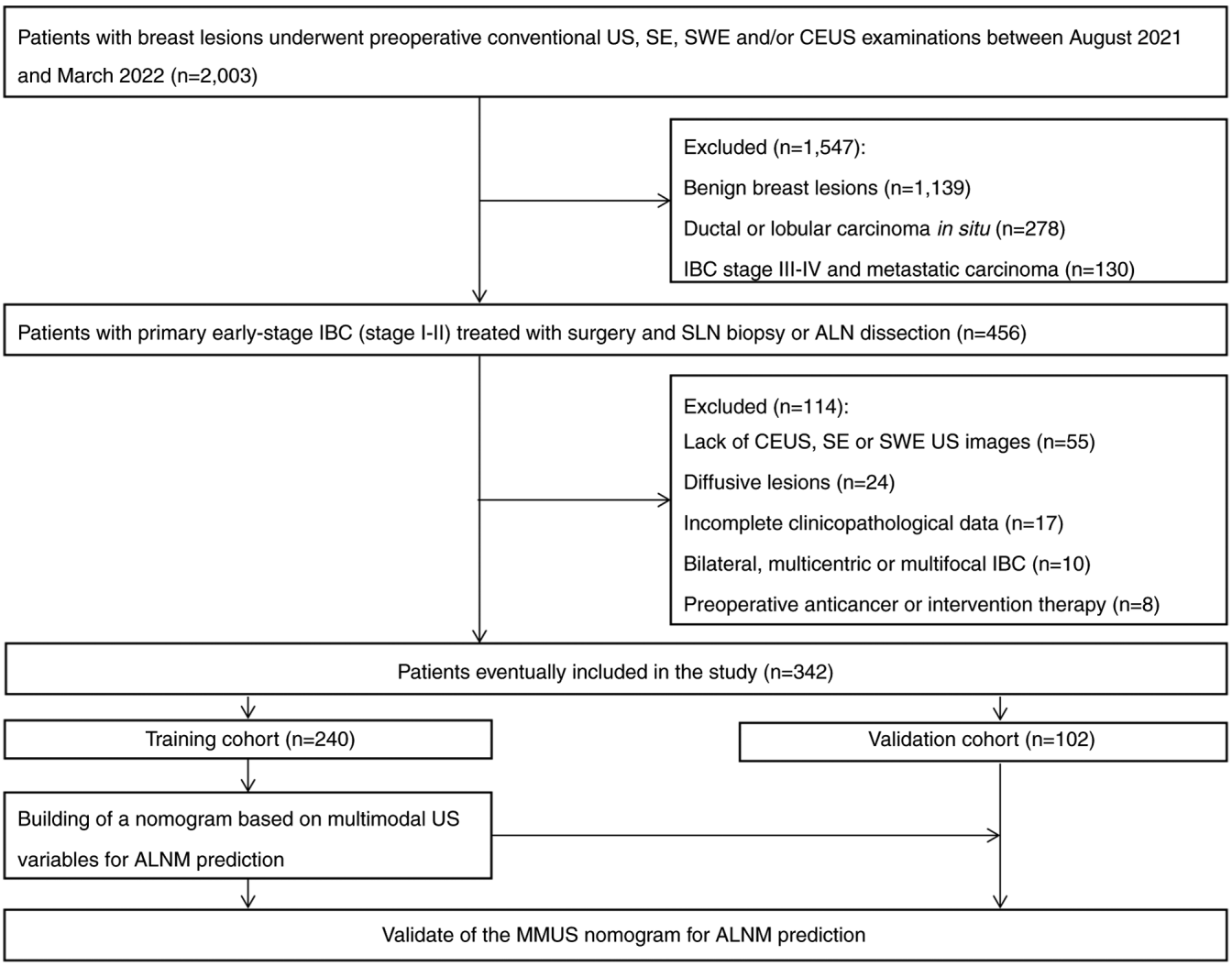

Figure 1. Patient recruitment and study design. SE, strain elastography; SWE, shear wave elastography; CEUS, contrast-enhanced ultrasound; IBC, invasive breast cancer; SLN, sentinel lymph node; ALNM, axillary LN metastasis; MMUS, multimodal US.

intensity reached its peak), peak intensity (PI; maximum intensity of the time-intensity curve), ascending slope (AS; slope from the beginning of focal perfusion to the peak point on the curve), descending slope (DS; curve descent slope) and area under the time-intensity curve (AUTIC; total volume of blood in the region of interest) were also recorded.

Observer variability for evaluation of the US features. In a subset of 60 randomly selected breast lesions and 30 ALNs, interobserver variability in conventional US, SE, SWE and CEUS of breast lesions and conventional US of ALNs were assessed separately by two radiologists (JJY and YZ). At 1 month after the first evaluation, one observer (JJY) reviewed all images of the same 60 lesions and 30 ALNs for the calculation of intra-observer variability.

Statistical analysis. Statistical analyses were performed using SPSS (version 25.0; IBM Corp.) and R software (version 4.1.3; The R Foundation). Continuous variables were compared using independent t-test. Categorical variables were compared using the χ^2 or Fisher's exact test. The Cohen κ statistic was used to assess interobserver agreement. All clinicopathological factors and conventional US features potentially associated with ALNM ($P<0.05$ in univariate analysis) were used to construct a clinicopathological model and a conventional US model. A nomogram was formulated based on multimodal US variables by the results of multivariate logistic analysis. Calibration was assessed using the calibration curve with 1,000 bootstrap samples to decrease overfit bias. The predictive performances were compared with AUC. Additionally, net reclassification improvement (NRI) was applied to evaluate incremental value, and decision curve analysis (DCA) to investigate the clinical usefulness of the nomogram. The 'rms' package was used for nomogram and calibration curve construction, the 'rmda' package for DCA and the 'nricens' package was used for NRI calculation. All packages were performed from R software (version 4.1.3; The R Foundation). $P<0.05$ was considered to indicate a statistically significant difference.

Results

Clinicopathological characteristics. A total of 342 patients were finally included in the present study and were randomly divided into the training (n=240) and validation (n=102)

Table I. Univariate analysis of clinical and pathological characteristics associated with axillary lymph node status.

A, Training cohort (n=240)

Characteristic	Axillary lymph node status		P-value
	Negative (n=155)	Positive (n=85)	
Age, years (%)	47.05±10.23	54.10±11.34	<0.001
<40	24 (15.48)	16 (18.82)	
40-60	99 (63.87)	30 (35.30)	
>60	32 (20.65)	39 (45.88)	
Symptoms (%)			0.338
Palpable mass	136 (87.74)	78 (91.76)	
Other	19 (12.26)	7 (8.24)	
Family history of breast cancer (%)			0.507
No	125 (80.65)	65 (76.47)	
Yes	30 (19.35)	20 (23.53)	
History of hormone therapy (%)			0.390
No	124 (80.00)	72 (84.71)	
Yes	31 (20.00)	13 (15.29)	
Clinical T stage (%)			0.043
T1	94 (60.65)	40 (47.06)	
T2	61 (39.35)	45 (52.94)	
Histological type (%)			0.874
Ductal	123 (79.35)	69 (81.18)	
Lobular or mixed	27 (17.42)	13 (15.29)	
Other	5 (3.23)	3 (3.53)	
Histological grade (%)			0.002
Low	11 (7.09)	5 (5.88)	
Intermediate	85 (54.84)	26 (30.59)	
High	59 (38.07)	54 (63.53)	
ER status (%)			0.868
Negative	27 (17.42)	14 (16.47)	
Positive	128 (82.58)	71 (83.53)	
PR status (%)			0.990
Negative	40 (25.81)	22 (25.88)	
Positive	115 (74.19)	63 (74.12)	
HER2 status (%)			0.885
Negative	123 (79.35)	57 (67.06)	
Positive	32 (20.65)	28 (32.94)	
Ki67 levels (%)			0.746
≤20%	45 (29.03)	23 (27.06)	
>20%	110 (70.97)	62 (72.94)	
Molecular subtype (%)			0.883
Luminal A	28 (18.06)	16 (18.82)	
Luminal B	95 (61.29)	51 (60.00)	
HER2-positive	23 (14.84)	11 (12.94)	
Triple negative	9 (5.81)	7 (8.24)	

Table I. Continued.

B, Validation cohort (n=102)

Characteristic	Axillary lymph node status		P-value
	Negative (n=64)	Positive (n=38)	
Age, years (%)	48.21±11.51	54.37±12.00	<0.001
<40	10 (15.63)	7 (18.42)	0.027
40-60	37 (57.81)	12 (31.58)	
>60	17 (26.56)	19 (50.00)	
Symptoms (%)			0.765
Palpable mass	56 (87.50)	34 (89.47)	
Other	8 (12.50)	4 (10.53)	
Family history of breast cancer (%)			0.922
No	50 (78.13)	30 (78.95)	
Yes	14 (21.87)	8 (21.05)	
History of hormone therapy (%)			0.804
No	51 (79.69)	29 (76.32)	
Yes	13 (20.31)	9 (23.68)	
Clinical T stage (%)			0.036
T1	40 (62.50)	16 (42.11)	
T2	24 (37.50)	22 (57.89)	
Histological type (%)			0.971
Ductal	51 (79.69)	31 (81.58)	
Lobular or mixed	11 (17.19)	6 (15.79)	
Other	2 (3.12)	1 (2.63)	
Histological grade (%)			0.026
Low	5 (7.81)	2 (5.26)	
Intermediate	35 (54.69)	12 (31.58)	
High	24 (37.50)	24 (63.16)	
ER status (%)			0.967
Negative	12 (18.75)	7 (18.42)	
Positive	52 (81.25)	31 (81.58)	
PR status (%)			0.747
Negative	17 (26.56)	8 (21.05)	
Positive	47 (73.43)	30 (78.95)	
HER2 status (%)			0.937
Negative	45 (70.31)	27 (71.05)	
Positive	19 (29.69)	11 (28.95)	
Ki67 levels (%)			0.929
≤20%	18 (28.13)	11 (28.95)	
>20%	46 (71.87)	27 (71.05)	
Molecular subtype (%)			0.953
Luminal A	12 (18.75)	6 (15.79)	
Luminal B	38 (59.38)	23 (60.53)	
HER2-positive	9 (14.06)	5 (13.16)	
Triple negative	5 (7.81)	4 (10.52)	

Data are presented as mean ± standard deviation. T stage, tumor stage; ER, estrogen receptor; PR, progesterone receptor; HER2, human epidermal growth factor receptor 2.

cohorts (Fig. 1). There were no significant differences in ALN positivity between cohorts [training cohort, 35.4% (85/240); validation cohort, 37.3% (38/102)]. The clinicopathological and US variables were not significantly different between cohorts, demonstrating no selection bias in the random allocation process.

Predictive factors associated with ALNM. Table I presents the distribution of clinicopathological characteristics in relation to ALN status. The results revealed that older age, clinical T2 stage compared with T1 stage, and high histological grade compared with low or intermediate grade were significantly more likely to be associated with ALNM in both cohorts. The other clinicopathological factors, such as symptoms, family history of BC, history of hormone therapy, ER, PR and HER2 status, Ki67 levels and molecular subtypes showed no significant differences between the ALN-positive and -negative groups. Univariate analysis of conventional US features revealed that tumors with a larger maximum size, heterogeneous echogenicity in comparison with homogeneous echogenicity, tumor with calcification in comparison with no calcification, high vascularity in comparison with absent or low vascularity and BI-RADS category 5 in comparison with BI-RADS category 3-4C were risk factors significantly associated with ALNM. However, tumor shape, margin, orientation and posterior acoustic pattern showed no significant predictive value for ALNM. In the training cohort, US-depicted suspicious ALN positive were 65 patients, the pathological results of ALNM were 85 patients, thus the diagnostic sensitivity was 76.47% (65/85). US-depicted suspicious ALN negative were 102 patients, the pathological results of ALN negative were 155 patients, thus the diagnostic specificity was 65.80% (102/155). In the validation cohort, US-depicted suspicious ALN positive were 30 patients, the pathological results of ALNM were 38 patients, the diagnostic sensitivity was 78.95% (30/38). US-depicted suspicious ALN negative were 41 patients, the pathological results of ALN negative were 64 patients, the diagnostic specificity was 64.06% (41/64) (Table II).

Additionally, the presence of stiff rim sign, perfusion defect and radial vessel in comparison with absent were also risk factors significantly associated with ALNM. However, the other MMUS variables, including SE features, E_{max}, E_{mean}, E_{min}, E_{SD}, AT, TTP, PI, AS, DS and AUTIC, demonstrated no significant association with ALNM (Table III).

The variables significantly associated with ALNM in univariate analysis were further evaluated by multivariate logistic analysis. The maximum tumor size [odds ratio (OR), 4.312; 95% CI, 2.933-7.364], heterogeneous echogenicity (OR, 2.473; 95% CI, 1.065-6.518), stiff rim sign (OR, 6.140; 95% CI, 3.202-15.893), perfusion defect (OR, 3.632; 95% CI, 0.772-8.644), radial vessel (OR, 7.577; 95% CI, 3.750-20.605) and US BI-RADS category 5 (OR, 8.178; 95% CI, 3.930-22.307) were independent risk factors significantly associated with ALNM (Table IV).

The interobserver agreement was substantial for breast tumor features of conventional US, SE, SWE and CEUS, with κ values of 0.840, 0.796, 0.827 and 0.801, respectively. For ALN status, κ value was 0.865. The intra-observer agreement was favorable, with κ values of 0.890 and 0.915 for breast tumor US features and ALN status, respectively.

Table II. Univariate analysis of conventional ultrasound features associated with axillary lymph node status.

A, Training cohort (n=240)

Feature	Axillary lymph node status: Negative (n=155)	Axillary lymph node status: Positive (n=85)	P-value
Maximum size, cm	2.21±1.20	2.93±1.82	<0.001
<2	38 (24.52)	4 (4.71)	<0.001
2-3	94 (60.64)	25 (29.41)	
3-5	23 (14.84)	56 (65.88)	
Shape (%)			0.366
Oval/round	39 (25.16)	17 (20.00)	
Irregular	116 (74.84)	68 (80.00)	
Margin (%)			0.538
Circumscribed	20 (12.90)	8 (9.41)	
Indistinct	58 (37.42)	33 (38.82)	
Angulation	45 (29.03)	24 (28.24)	
Microlobulation	9 (5.81)	6 (7.06)	
Spiculation	23 (14.84)	14 (16.47)	
Orientation (%)			0.691
Parallel	136 (87.74)	77 (90.59)	
Not parallel	19 (12.26)	8 (9.41)	
Echogenicity			<0.001
Homogeneous	110 (70.97)	19 (22.35)	
Heterogeneous	45 (29.03)	66 (77.65)	
Posterior acoustic (%)			0.270
No change	39 (25.16)	17 (20.00)	
Enhancement	23 (14.84)	21 (24.70)	
Mixed change	33 (21.29)	15 (17.65)	
Shadow	60 (38.71)	32 (37.65)	
Calcification (%)			<0.001
Absent	117 (75.48)	35 (41.18)	
Present	38 (24.52)	50 (58.82)	
Vascularity (%)			0.002
Absent/low	60 (38.71)	16 (18.82)	
High	95 (61.29)	69 (81.18)	
BI-RADS category (%)			<0.001
3	3 (1.94)	1 (1.18)	
4A	24 (15.48)	6 (7.06)	
4B	40 (25.81)	13 (15.29)	
4C	59 (38.06)	23 (27.06)	
5	29 (18.71)	42 (49.41)	
US-depicted suspicious ALN (%)			<0.001
Negative	102 (65.81)	20 (23.53)	
Positive	53 (34.19)	65 (76.47)	

Table II. Continued.

B, Validation cohort (n=102)

Feature	Axillary lymph node status		P-value
	Negative (n=64)	Positive (n=38)	
Maximum size, cm (%)	2.14±1.32	3.20±1.90	<0.001
<2	14 (21.88)	2 (5.26)	<0.001
2-3	40 (62.50)	10 (26.32)	
4-5	10 (15.62)	26 (68.42)	
Shape (%)			0.677
Oval/round	14 (21.88)	7 (18.42)	
Irregular	50 (78.12)	31 (81.58)	
Margin (%)			0.645
Circumscribed	6 (9.38)	4 (10.53)	
Indistinct	24 (37.50)	13 (34.21)	
Angulation	17 (26.56)	10 (26.32)	
Microlobulation	4 (6.25)	3 (7.89)	
Spiculation	13 (20.31)	8 (21.05)	
Orientation (%)			0.734
Parallel	54 (84.4)	33 (86.84)	
Not parallel	10 (15.6)	5 (13.16)	
Echogenicity (%)			<0.001
Homogeneous	45 (70.31)	8 (21.05)	
Heterogeneous	19 (29.69)	30 (78.95)	
Posterior acoustic (%)			0.489
No change	15 (23.44)	7 (18.42)	
Enhancement	9 (14.06)	10 (26.32)	
Mixed change	14 (21.88)	7 (18.42)	
Shadow	26 (40.62)	14 (36.84)	
Calcification (%)			0.002
Absent	45 (70.31)	15 (39.47)	
Present	19 (29.69)	23 (60.53)	
Vascularity (%)			0.019
Absent/low	23 (35.94)	6 (15.79)	
High	41 (64.06)	32 (84.21)	
BI-RADS category (%)			<0.001
3	2 (3.13)	1 (2.63)	
4A	12 (18.75)	2 (5.26)	
4B	15 (23.44)	6 (15.79)	
4C	25 (39.06)	10 (26.32)	
5	10 (15.62)	19 (50.00)	
US-depicted suspicious ALN (%)			<0.001
Negative	41 (64.06)	8 (21.05)	
Positive	23 (35.94)	30 (78.95)	

Data are presented as mean ± standard deviation. BI-RADS, Breast Imaging and Reporting Data System; US, ultrasound; ALN, axillary lymph node.

Nomogram development and validation. MMUS nomogram was constructed based on the six independent risk factors determined by multivariate logistic analysis. Probability of ALNM was obtained by summing corresponding points from these predictive variables (Fig. 2A). The calibration curve with 1,000 bootstrap samples demonstrated a high level of consistency between MMUS nomogram predictions and actual ALNM probabilities in both the training and validation cohorts (Fig. 2B and C). Moreover, MMUS nomogram showed a favorable prediction efficacy, with AUCs of 0.927 and 0.922 in the training and validation cohorts, respectively.

Discrimination and clinical usefulness of MMUS nomogram. A clinicopathological model and conventional US model were constructed to compare the predictive effect of ALNM. The clinicopathological model was built with age, clinical tumor (T) stage and histological grade, while the conventional US model was built with maximum tumor size, echogenicity, calcification, vascularity and US BI-RADS category. ROCs of the two models and the MMUS nomogram in both cohorts are shown in Fig. 3. MMUS nomogram demonstrated an improved predictive performance (AUC, 0.927; 95% CI, 0.891, 0.973) compared with that of the clinicopathological model (AUC, 0.681; 95% CI, 0.594, 0.740), US-depicted ALN status (AUC, 0.710; 95% CI, 0.643, 0.780) and conventional US model (AUC, 0.867; 95% CI, 0.837, 0.904) in the training cohort. In the validation cohort, AUCs were 0.922 (95% CI, 0.880, 0.962), 0.670 (95% CI, 0.588, 0.723), 0.716 (95% CI, 0.693, 0.796) and 0.894 (95% CI, 0.851, 0.924), respectively. The NRI index, which determined performance improvement as introduced by multimodal US features in the conventional US model, was 0.296 (95% CI, 0.084, 0.385) in the training cohort and 0.288 (95% CI, 0.069, 0.361) in the validation cohort. DCA demonstrated that the MMUS nomogram achieved an improved benefit and clinical utility in predicting ALNM for patients with early-stage IBC when high-risk threshold probability was 0.0-1.0 (Fig. 4).

Discussion

SLN biopsy is known to have multiple complications owing to its invasive process and false-negative rates of 7.8-27.3% (27,28). Therefore, there have been efforts to establish a non-invasive mathematical model to replace SLN biopsy in determining preoperative ALN status. Previous studies have reported that conventional US, SE, SWE US or CEUS methods serve an important role in prediction of tumor growth or metastasis (13,29-31). However, to the best of our knowledge, the present study is the first to construct a MMUS nomogram based on a set of comprehensive multimodal US features of primary breast tumor to predict ALNM. The MMUS nomogram achieved the most favorable performance compared with the clinicopathological model, US-depicted ALN status and conventional US model (AUC of 0.922 vs. 0.670, 0.716 and 0.894 in the validation cohort). Furthermore, MMUS nomogram was a useful predictive model for calibration and DCA.

It is known that clinical and pathological characteristics serve an important role in prognosis prediction (32,33). A study by The Memorial Sloan-Kettering Cancer Center (MSKCC) developed a clinicopathological model (MSKCC

Table III. Univariate analysis of SE, SWE and contrast-enhanced ultrasound features associated with axillary lymph node status.

A, Training cohort (n=240)

Feature	Axillary lymph node status		P-value
	Negative (n=155)	Positive (n=85)	
SE (%)			0.817
Soft	22 (14.19)	13 (15.29)	
Hard	133 (85.81)	72 (84.71)	
Stiff rim sign (%)			<0.001
Absent	105 (67.74)	25 (29.41)	
Present	50 (32.26)	60 (70.59)	
SWE, kPa			0.764
E_{max}	135.15±31.08	133.19±29.35	
E_{min}	3.72±1.85	3.61±1.71	
E_{mean}	24.55±8.91	22.23±8.06	
E_{SD}	18.26±7.69	17.54±7.15	
Enhancement degree (%)			0.182
Hypo/isoenhancement	39 (25.16)	15 (17.65)	
Hyperenhancement	116 (74.84)	70 (82.35)	
Perfusion defect (%)			<0.001
Absent	116 (74.84)	25 (29.41)	
Present	39 (25.16)	60 (70.59)	
Radial vessel (%)			<0.001
Absent	109 (70.32)	19 (22.35)	
Present	46 (29.68)	66 (77.65)	
AT	0.55±0.28	0.51±0.23	0.756
TTP	11.93±3.87	13.12±4.24	0.675
PI	28.12±10.34	31.09±10.86	0.469
AS	2.38±1.79	2.25±1.61	0.780
DS	-0.47±0.21	-0.43±0.32	0.412
AUTIC	2,819.56±887.12	2,967.41±923.04	0.312

B, Validation cohort (n=102)

Feature	Axillary lymph node status		P-value
	Negative (n=64)	Positive (n=38)	
SE (%)			0.734
Soft	10 (15.63)	5 (13.16)	
Hard	54 (84.37)	33 (86.84)	
Stiff rim sign (%)			<0.001
Absent	44 (68.75)	11 (28.95)	
Present	20 (31.25)	27 (71.05)	
SWE, kPa			0.908
E_{max}	136.24±2.11	134.33±30.48	
E_{min}	3.81±1.79	3.76±1.68	
E_{mean}	26.89±9.57	25.72±7.87	
E_{SD}	20.14±8.13	18.78±7.91	
Enhancement degree (%)			0.359
Hypo/isoenhancement	13 (20.31)	5 (13.16)	
Hyperenhancement	51 (79.69)	33 (86.84)	

Table III. Continued.

B, Validation cohort (n=102)

Feature	Axillary lymph node status		P-value
	Negative (n=64)	Positive (n=38)	
Perfusion defect (%)			<0.001
Absent	45 (70.31)	10 (26.32)	
Present	19 (29.69)	28 (73.68)	
Radial vessel (%)			<0.001
Absent	47 (73.44)	9 (23.68)	
Present	17 (26.56)	29 (76.32)	
AT	0.54±0.25	0.52±0.20	0.821
TTP	11.14±3.96	12.88±4.01	0.761
PI	29.89±11.02	31.37±11.12	0.508
AS	2.40±1.87	2.31±1.70	0.843
DS	-0.46±0.19	-0.45±0.28	0.640
AUTIC	2,776.51±907.23	2,879.56±974.15	0.551

Data are presented as mean ± SD. SE, strain elastography; SWE, shear wave elastography; AT, arrival time; TTP, time to peak; PI, peak intensity; AS, ascending slope; DS, descending slope; AUTIC, area under the time-intensity curve.

Table IV. Multivariate logistic regression analysis of risk factors for predicting axillary lymph node metastasis in the training cohort.

Factor	B	OR	95% CI	P-value
Age, years	0.016	1.029	0.849-1.074	0.302
Clinical T stage, T2 vs. T1	-0.521	0.819	0.286-1.765	0.513
Histological grade, high vs. intermediate or low	1.187	2.279	0.991-5.438	0.271
Maximum size, cm	1.904	4.312	2.933-7.364	<0.001
Echogenicity, heterogeneous vs. homogeneous	1.245	2.473	1.065-6.518	0.039
Calcification, present vs. absent	-0.300	0.741	0.475-2.965	0.672
Vascularity, high vs. low or absent	-0.151	0.860	0.234-2.159	0.821
Stiff rim sign, present vs. absent	1.267	6.140	3.202-15.893	<0.001
Perfusion defect, present vs. absent	1.090	3.632	0.772-8.644	0.002
Radial vessel, present vs. absent	2.269	7.557	3.750-20.605	<0.001
US BI-RADS categories, 5 vs. 3-4C	1.432	8.178	3.930-22.307	<0.001

B, regression coefficient; OR, odds ratio; CI, confidence interval; T stage, tumor stage; US, ultrasound; BI-RADS, Breast Imaging and Reporting Data System.

nomogram) to predict SLN metastasis; however, AUC of the MSKCC nomogram was relatively low at 0.754 (32). Previous studies have reported that age, ER, PR and HER2 status have no effect in predicting ALNM in patients with early-stage BC (33-35). The present study demonstrated that older age, clinical T2 stage and high tumor grade were more likely to predict ALNM in the univariate analysis, but they were not independent risk factors associated with ALNM in the multivariate analysis. The clinicopathological model based on these three variables displayed low predictive probability with AUCs of 0.681 and 0.670 in the training and validation cohorts, respectively. These results indicated that the clinicopathological factors may not provide sufficient value in predicting ALN status, which is consistent with previous studies (33-36).

Conventional US features of breast tumor showed that larger tumor size, heterogeneous echogenicity, calcification, high vascularity and BI-RADS category 5 were potential risk factors associated with ALNM in the univariate analysis. These variables formed the conventional US predictive model, whereas calcification and high vascularity were not significantly associated with ALNM in the multivariate

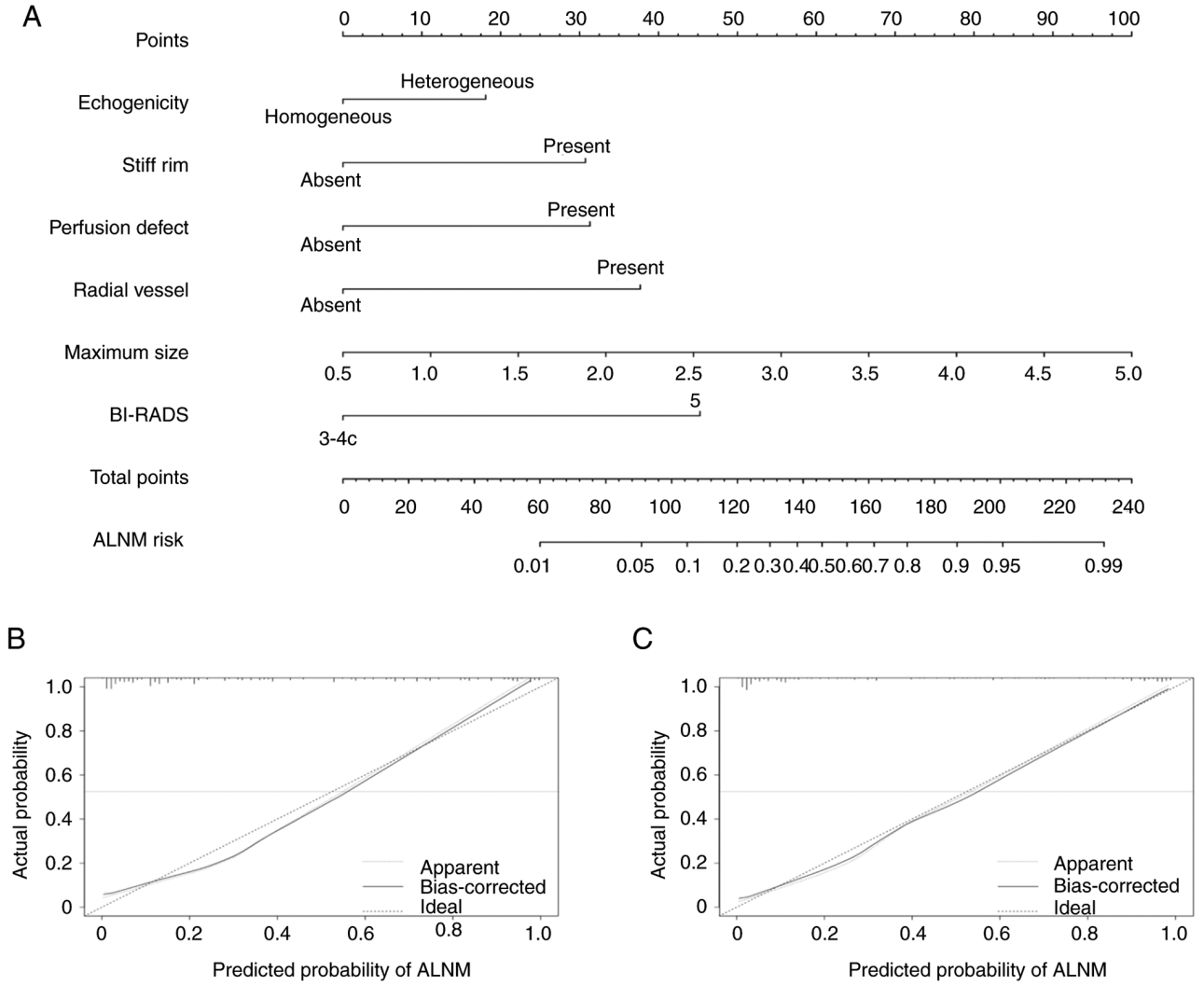

Figure 2. MMUS nomogram and calibration curves. (A) MMUS nomogram was developed with echogenicity, stiff rim sign, perfect defect, radial vessel, maximum size and BI-RADS category for the prediction of ALNM risk in the training cohort. To use the nomogram, the different values of each variable are corresponded to a point at the top of the graph and the total points to the bottom line is the probability of ALNM. The calibration curves of the MMUS nomogram in (B) training and (C) validation cohorts demonstrated agreement between actual ALNM rate (ideal) and predictive ALNM rate estimated by MMUS nomogram (solid line). MMUS, multimodal ultrasound; BI-RADS, Breast Imaging and Reporting Data System; ALNM, axillary lymph node metastasis, Predicted Pr[y=positive], Predicted probability of axillary lymph node positive.

analysis and were excluded from the final MMUS nomogram model. Larger tumor size, heterogeneous echogenicity and US BI-RADS category 5, as independent risk factors associated with ALNM, indicated that rapidly proliferating tumor cells with a larger tumor size tend to propagate within the regional lymph nodes (37,38). Heterogeneous echogenicity may be the result of genomic heterogeneity, which is a potential biomarker to predict metastasis (39). The more malignant US features the lesion has, the higher the BI-RADS category is, and the worse the prognosis may be (40,41).

US elastography enables differentiation of tissues to be made on the basis of their stiffness. The stiff rim sign in SWE, which represents increased stiffness at the lesion margin, is regarded as a sign of malignancy (12,25). It has been explained as either a desmoplastic reaction or infiltration of cancer cells into the peritumoral stroma (25,41). The results of the present study demonstrated that stiff rim sign was an independent prognostic factor associated with ALNM, consistent with previous studies (41,42). CEUS is a promising technology that can reflect the micro-circulation perfusion of breast lesions (30,31). In the present study, perfusion defect and radial vessel at the tumor margin were the best predictive factors associated with ALNM. When the SWE and CEUS features were combined with the conventional US variables to form the MMUS nomogram, the incremental value was demonstrated, with AUC improved from 0.894 to 0.922 and with NRI improved 0.288 in comparison with the conventional US model in the validation cohort. The results indicated that aggressive breast tumors require a higher level of angiogenesis to maintain growth and infiltration, peritumoral vessels can lead to local ALN or distant metastasis and intrinsic necrosis may be due to the relatively insufficient nutrition supply, which is manifested as a perfusion defect (31,37,38,43).

The present study demonstrated that the SE features and SWE (E_{mean}, E_{max}, E_{min} and E_{SD}) and CEUS quantitative parameters (AT, TTP, PI, AS, DS and AUTIC) had no

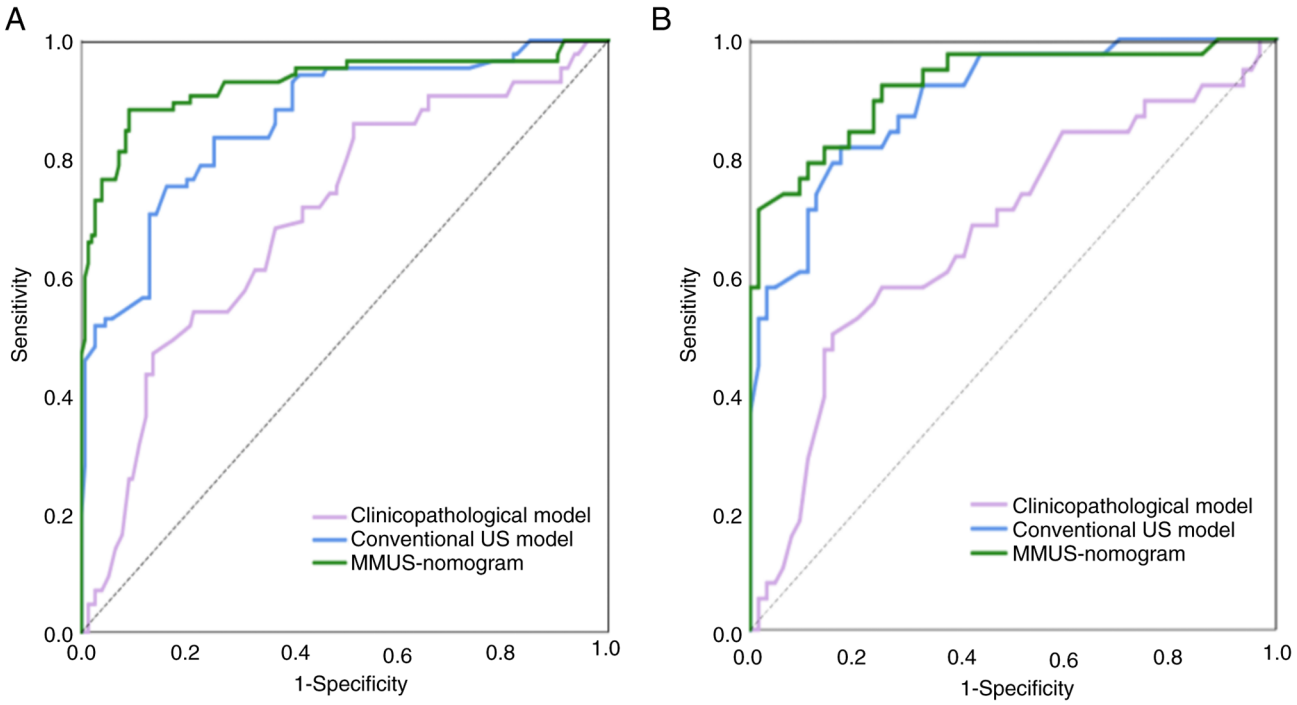

Figure 3. Area under the receiver operating characteristic curves in both cohorts. The area under the curves for the clinicopathological and conventional US model and the MMUS nomogram were 0.681, 0.867 and 0.927 in (A) training cohort and 0.670, 0.894 and 0.922 in the validation cohort (B). MMUS, multimodal ultrasound.

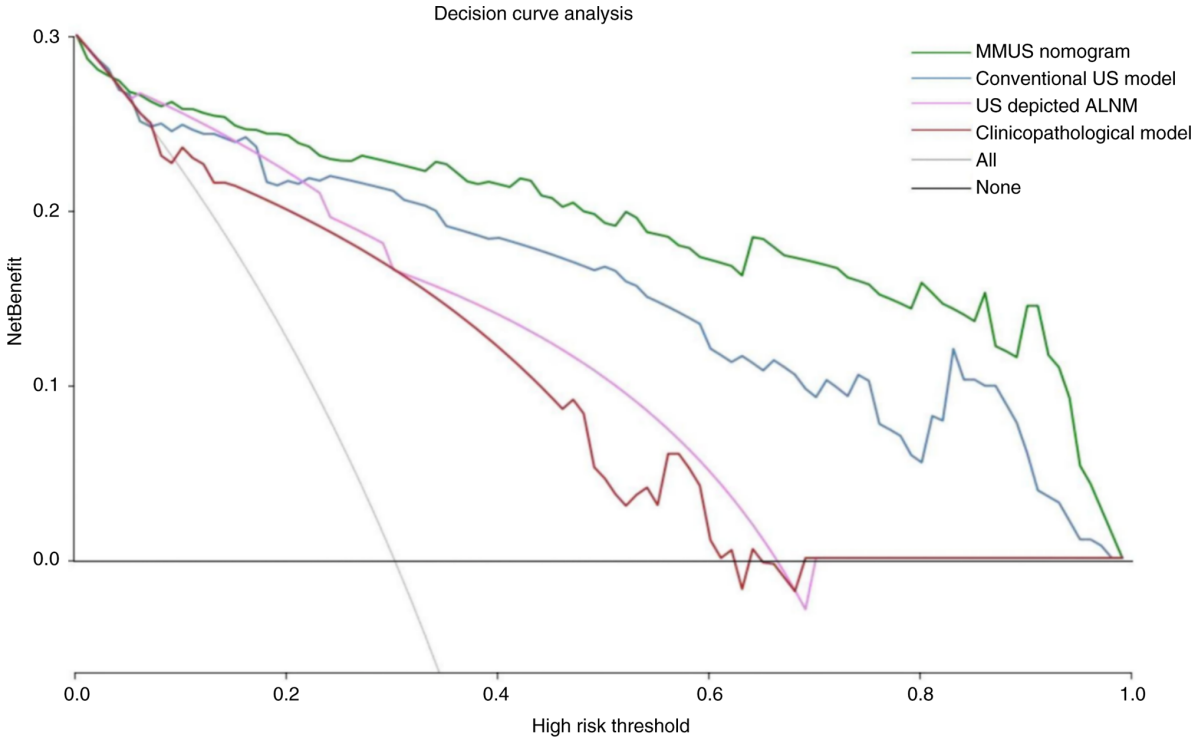

Figure 4. Decision curve analysis of MMUS nomogram, conventional US model, US-depicted ALN status and clinicopathological model for the prediction of ALNM. The gray line represents the assumption that all patients have ALNM (treat-all scheme). The black horizontal line represents the assumption that no patients have ALNM (treat-none scheme). If high-risk threshold probability is 0.0-1.0, using the MMUS nomogram for ALNM prediction achieves the greatest benefit. MMUS, multimodal ultrasound; ALNM, axillary lymph node metastasis.

significant predictive value for ALNM. These results were different from the results obtained by Zhang *et al* (41) who reported that E_{max} and E_{mean} of primary tumors are higher in ALNM cases, and Wan *et al* (30) who reported that ALNM is associated with higher PI and larger AUTIC values. These discrepancies may be due to inclusion criteria or

different US equipment and settings. Different US instruments have different sensitivities for detection of SWE and CEUS quantitative parameters (25,31,41,43), which may account for the inconsistent results. Further studies with larger and multicenter data are required to assess possible associations.

Certain limitations in the present study have to be addressed. The present study is limited by a lack of multicenter external validation patients. Although the nomogram achieved favorable predictive ability, selection bias was inevitable due to the retrospective nature of the study. Moreover, to analyze the association between tumor features and ALN status, patients with bilateral, multicentric or multifocal tumors were excluded and only one US equipment was used, which may also have caused selection bias. The present study did not distinguish the number of metastatic ALNs. Another study by our team in collaboration with external institutions was initiated to predict the burden of ALNM (44). Although the variability study was favorable in terms of features and parameters evaluated from the same images at different times, full analysis of variability, such as the acquirement of multiple images at different times and from different operators, is needed. Internal mammary lymph nodes were not evaluated. For patients with internal mammary lymph node metastasis, radiotherapy is necessary following surgery and the final pathological node status is difficult to determine (45). In addition, US is the most frequently used imaging modality in determining lymph node metastasis in daily clinical practice (29-31). Nomograms are a simple, intuitive and easy to understand risk scoring tool represented by graphs (32). MMUS nomogram in the present study achieved favorable diagnostic performance and may facilitate clinicians in appropriate preoperative decision-making. Previous researchers have reported that standard breast magnetic resonance imaging (MRI) is comparable with dedicated axillary US for evaluation of axillary nodal status in patients with BC (46,47). However, the comparison of MMUS nomogram with enhanced MRI in determining lymph node metastasis was not performed in the present study and further studies are required to address this issue in the future. However, despite the aforementioned limitations, the present study had adequate sample size and a well-characterized cohort of patients with early-stage IBC with a large series of combined multimodal US features of each breast tumor and the nomogram represented an easy-to-use predictive tool with favorable diagnostic performance. Moreover, application of the MMUS nomogram in everyday clinical practice may be simpler compared with other types of radiomics and deep learning analyses.

In conclusion, the present study demonstrated that the MMUS nomogram was superior to US-depicted ALN status and clinicopathological and conventional US model for the prediction of ALNM. As a non-invasive, convenient, comprehensive and reliable predictive tool, the MMUS nomogram may facilitate appropriate preoperative decision-making for patients with early-stage IBC.

Acknowledgements

Not applicable.

Funding

No funding was received.

Availability of data and materials

The data generated in the present study may be requested from the corresponding author.

Authors' contributions

JJY, WZ and WWZ were responsible for study conception and design. WZ contributed to manuscript preparation and editing. JJY and YZ performed ultrasonographic data analysis and interpretation. XSC collected and interpreted clinicopathological data. JQZ contributed to the statistical analysis. WZ and WWZ confirm the authenticity of all the raw data. All authors have read and approved the final manuscript.

Ethics approval and consent to participate

The present study was approved by and conducted in accordance with the Declaration of Helsinki and approved by the Ethics Committee of Ruijin Hospital, School of Medicine, Shanghai Jiao Tong University (Shanghai, China; approval no. 2020-309; July 15, 2020). Written informed consent were obtained from patients to participate in the study.

Patient consent for publication

Not applicable.

Competing interests

The authors declare that they have no competing interests.

References

1. Sung H, Ferlay J, Siegel RL, Laversanne M, Soerjomataram I, Jemal A and Bray F: Global cancer statistics 2020: GLOBOCAN estimates of incidence and mortality worldwide for 36 cancers in 185 countries. CA Cancer J Clin 71: 209-249, 2021.
2. Giuliano AE, Ballman KV, McCall L, Beitsch PD, Brennan MB, Kelemen PR, Ollila DW, Hansen NM, Whitworth PW, Blumencranz PW, *et al*: Effect of axillary dissection vs. no axillary dissection on 10-year overall survival among women with invasive breast cancer and sentinel node metastasis: The ACOSOG Z0011 (alliance) randomized clinical trial. JAMA 318: 918-926, 2017.
3. Lyman GH, Somerfield MR, Bosserman LD, Perkins CL, Weaver DL and Giuliano AE: Sentinel lymph node biopsy for patients with early-stage breast cancer: American society of clinical oncology clinical practice guideline update. J Clin Oncol 35: 561-564, 2017.
4. Wilke LG, McCall LM, Posther KE, Whitworth PW, Reintgen DS, Leitch AM, Gabram SG, Lucci A, Cox CE, Hunt KK, *et al*: Surgical complications associated with sentinel lymph node biopsy: Results from a prospective international cooperative group trial. Ann Surg Oncol 13: 491-500, 2006.
5. Manca G, Rubello D, Tardelli E, Giammarile F, Mazzarri S, Boni G, Chondrogiannis S, Marzola MC, Chiacchio S, Ghilli M, *et al*: Sentinel lymph node biopsy in breast cancer: Indications, contraindications, and controversies. Clin Nucl Med 41: 126-133, 2016.

6. Zhang YN, Wang CJ, Xu Y, Zhu QL, Zhou YD, Zhang J, Mao F, Jiang YX and Sun Q: Sensitivity, specificity and accuracy of ultrasound in diagnosis of breast cancer metastasis to the axillary lymph nodes in Chinese patients. Ultrasound Med Biol 41: 1835-1841, 2015.
7. Hotton J, Salleron J, Henrot P, Buhler J, Leufflen L, Rauch P and Marchal F: Pre-operative axillary ultrasound with fine-needle aspiration cytology performance and predictive factors of false negatives in axillary lymph node involvement in early breast cancer. Breast Cancer Res Treat 183: 639-647, 2020.
8. Yu FH, Wang JX, Ye XH, Deng J, Hang J and Yang B: Ultrasound-based radiomics nomogram: A potential biomarker to predict axillary lymph node metastasis in early-stage invasive breast cancer. Eur J Radiol 119: 108658, 2019.
9. Qiu X, Jiang Y, Zhao Q, Yan C, Huang M and Jiang T: Could ultrasound-based radiomics noninvasively predict axillary lymph node metastasis in breast cancer? J Ultrasound Med 39: 1897-1905, 2020.
10. Jiang M, Li CL, Luo XM, Chuan ZR, Chen RX, Tang SC, Lv WZ, Cui XW and Dietrich CF: Radiomics model based on shear-wave elastography in the assessment of axillary lymph node status in early-stage breast cancer. Eur Radiol 32: 2313-2325, 2022.
11. Lee S, Jung Y and Bae Y: Clinical application of a color map pattern on shear-wave elastography for invasive breast cancer. Surg Oncol 25: 44-48, 2016.
12. Tozaki M and Fukuma E: Pattern classification of ShearWave™ elastography images for differential diagnosis between benign and malignant solid breast masses. Acta Radiol 52: 1069-1075, 2011.
13. Evans A, Whelehan P, Thomson K, McLean D, Brauer K, Purdie C, Baker L, Jordan L, Rauchhaus P and Thompson A: Invasive breast cancer: Relationship between shear-wave elastographic findings and histologic prognostic factors. Radiology 263: 673-677, 2012.
14. Huang R, Lin Z, Dou H, Wang J, Miao J, Zhou G, Jia X, Xu W, Mei Z, Dong Y, *et al*: AW3M: An auto-weighting and recovery framework for breast cancer diagnosis using multi-modal ultrasound. Med Image Anal 72: 102137, 2021.
15. Zheng X, Yao Z, Huang Y, Yu Y, Wang Y, Liu Y, Mao R, Li F, Xiao Y, Wang Y, *et al*: Deep learning radiomics can predict axillary lymph node status in early-stage breast cancer. J Nat Commun 11: 1236, 2020.
16. Guo X, Liu Z, Sun C, Zhang L, Wang Y, Li Z, Shi J, Wu T, Cui H, Zhang J, *et al*: Deep learning radiomics of ultrasonography: Identifying the risk of axillary non-sentinel lymph node involvement in primary breast cancer. EBioMedicine 60: 103018, 2020.
17. Liu D, Wu J, Lin C, Ding S, Lu S, Fang Y, Huang J, Hong J, Gao W, Zhu S, *et al*: The comparative safety of epirubicin and cyclophosphamide versus docetaxel and cyclophosphamide in lymph node-negative, HR-positive, HER2-negative breast cancer (ELEGANT): A randomized trial. Cancers (Basel) 14: 3221, 2022.
18. Collins GS, Reitsma JB, Altman DG and Moons KG: Transparent reporting of a multivariable prediction model for individual prognosis or diagnosis (TRIPOD): The TRIPOD statement. Br J Surg 102: 148-158, 2015.
19. Penault-Llorca F, André F, Sagan C, Lacroix-Triki M, Denoux Y, Verriele V, Jacquemier J, Baranzelli MC, Bibeau F, Antoine M, *et al*: Ki67 expression and docetaxel efficacy in patients with estrogen receptor-positive breast cancer. J Clin Oncol 27: 2809-2815, 2009.
20. Coates AS, Winer EP, Goldhirsch A, Gelber RD, Gnant M, Piccart-Gebhart M, Thürlimann B and Senn HJ; Panel Members: Tailoring therapies-improving the management of early breast cancer: St Gallen international expert consensus on the primary therapy of early breast cancer 2015. Ann Oncol 26: 1533-1546, 2015.
21. Mercado CL: BI-RADS update. Radiol Clin North Am 52: 481-487, 2014.
22. Bedi DG, Krishnamurthy R, Krishnamurthy S, Edeiken BS, Le-Petross H, Fornage BD, Bassett RL Jr and Hunt KK: Cortical morphologic features of axillary lymph nodes as a predictor of metastasis in breast cancer: In vitro sonographic study. AJR Am J Roentgenol 191: 646-652, 2008.
23. Koelliker SL, Chung MA, Mainiero MB, Steinhoff MM and Cady B: Axillary lymph nodes: US-guided fine-needle aspiration for initial staging of breast cancer-correlation with primary tumor size. Radiology 246: 81-89, 2008.
24. Itoh A, Ueno E, Tohno E, Kamma H, Takahashi H, Shiina T, Yamakawa M and Matsumura T: Breast disease: Clinical application of US elastography for diagnosis. Radiology 239: 341-350, 2006.
25. Zhou J, Zhan W, Chang C, Zhang X, Jia Y, Dong Y, Zhou C, Sun J and Grant EG: Breast lesions: Evaluation with shear wave elastography, with special emphasis on the 'stiff rim' sign. Radiology 272: 63-72, 2014.
26. Sidhu PS, Cantisani V, Dietrich CF, Gilja OH, Saftoiu A, Bartels E, Bertolotto M, Calliada F, Clevert DA, Cosgrove D, *et al*: The EFSUMB guidelines and recommendations for the clinical practice of contrast-enhanced ultrasound (CEUS) in non-hepatic applications: Update 2017 (long version). Ultraschall Med 39: e2-e44, 2018.
27. Li H, Jun Z, Zhi-Cheng G and Xiang Q: Factors that affect the false negative rate of sentinel lymph node mapping with methylene blue dye alone in breast cancer. J Int Med Res 47: 4841-4853, 2019.
28. Pesek S, Ashikaga T, Krag LE and Krag D: The false-negative rate of sentinel node biopsy in patients with breast cancer: A meta-analysis. World J Surg 36: 2239-2251, 2012.
29. Fang J, Zhao W, Li Q, Zhang B, Pu C and Wang H: Correlation analysis of conventional ultrasound characteristics and strain elastography with ki-67 status in breast cancer. Ultrasound Med Biol 46: 2972-2978, 2020.
30. Wan CF, Du J, Fang H, Li FH, Zhu JS and Liu Q: Enhancement patterns and parameters of breast cancers at contrast-enhanced US: Correlation with prognostic factors. Radiology 262: 450-459, 2012.
31. Zhu AQ, Li XL, An LW, Guo LH, Fu HJ, Sun LP and Xu HX: Predicting axillary lymph node metastasis in patients with breast invasive ductal carcinoma with negative axillary ultrasound results using conventional ultrasound and contrast-enhanced ultrasound. J Ultrasound Med 39: 2059-2070, 2020.
32. Bevilacqua JL, Kattan MW, Fey JV, Cody HS III, Borgen PI and Van Zee KJ: Doctor, what are my chances of having a positive sentinel node? A validated nomogram for risk estimation. J Clin Oncol 25: 3670-3679, 2007.
33. Yoshihara E, Smeets A, Laenen A, Reynders A, Soens J, Van Ongeval C, Moerman P, Paridaens R, Wildiers H, Neven P and Christiaens MR: Predictors of axillary lymph node metastases in early breast cancer and their applicability in clinical practice. Breast 22: 357-361, 2013.
34. Xiong J, Zuo W, Wu Y, Wang X, Li W, Wang Q, Zhou H, Xie M and Qin X: Ultrasonography and clinicopathological features of breast cancer in predicting axillary lymph node metastases. BMC Cancer 22: 1155, 2022.
35. Yu Y, Tan Y, Xie C, Hu Q, Ouyang J, Chen Y, Gu Y, Li A, Lu N, He Z, *et al*: Development and validation of a preoperative magnetic resonance imaging radiomics-based signature to predict axillary lymph node metastasis and disease-free survival in patients with early-stage breast cancer. JAMA Netw Open 3: e2028086, 2020.
36. Dong Y, Feng Q, Yang W, Lu Z, Deng C, Zhang L, Lian Z, Liu J, Luo X, Pei S, *et al*: Preoperative prediction of sentinel lymph node metastasis in breast cancer based on radiomics of T2-weighted fat-suppression and diffusion-weighted MRI. Eur Radiol 28: 582-591, 2018.
37. Fujii T, Yajima R, Tatsuki H, Suto T, Morita H, Tsutsumi S and Kuwano H: Significance of lymphatic invasion combined with size of primary tumor for predicting sentinel lymph node metastasis in patients with breast cancer. Anticancer Res 35: 3581-3584, 2015.
38. Auvinen P, Tammi R, Parkkinen J, Tammi M, Agren U, Johansson R, Hirvikoski P, Eskelinen M and Kosma VM: Hyaluronan in peritumoral stroma and malignant cells associates with breast cancer spreading and predicts survival. Am J Pathol 156: 529-536, 2000.
39. Bae MS, Shin SU, Song SE, Ryu HS, Han W and Moon WK: Association between US features of primary tumor and axillary lymph node metastasis in patients with clinical T1-T2N0 breast cancer. Acta Radiol 59: 402-408, 2018.
40. Sheng DL, Shen XG, Shi ZT, Chang C and Li JW: Survival outcome assessment for triple-negative breast cancer: A nomogram analysis based on integrated clinicopathological, sonographic, and mammographic characteristics. Eur Radiol 32: 6575-6587, 2022.
41. Zhang H, Dong Y, Jia X, Zhang J, Li Z, Chuan Z, Xu Y, Hu B, Huang Y, Chang C, *et al*: Comprehensive risk system based on shear wave elastography and BI-RADS categories in assessing axillary lymph node metastasis of invasive breast cancer-A multi-center study. Front Oncol 12: 830910, 2022.

42. Evans A, Rauchhaus P, Whelehan P, Thomson K, Purdie CA, Jordan LB, Michie CO, Thompson A and Vinnicombe S: Does shear wave ultrasound independently predict axillary lymph node metastasis in women with invasive breast cancer? Breast Cancer Res Treat 143: 153-157, 2014.
43. Matsubayashi R, Matsuo Y, Edakuni G, Satoh T, Tokunaga O and Kudo S: Breast masses with peripheral rim enhancement on dynamic contrast-enhanced MR images: Correlation of MR findings with histologic features and expression of growth factors. Radiology 217: 841-848, 2000.
44. Yao J, Zhou W, Xu S, Jia X, Zhou J, Chen X and Zhan W: Machine learning-based breast tumor ultrasound radiomics for pre-operative prediction of axillary sentinel lymph node metastasis burden in early-stage invasive breast cancer. Ultrasound Med Biol 50: 229-236, 2024.
45. Yang K, Kim H, Choi DH, Park W, Noh JM and Cho WK: Optimal radiotherapy for patients with internal mammary lymph node metastasis from breast cancer. Radiat Oncol 15: 16, 2020.
46. van Nijnatten TJA, Ploumen EH, Schipper RJ, Goorts B, Andriessen EH, Vanwetswinkel S, Schavemaker M, Nelemans P, de Vries B, Beets-Tan RGH, *et al*: Routine use of standard breast MRI compared to axillary ultrasound for differentiating between no, limited and advanced axillary nodal disease in newly diagnosed breast cancer patients. Eur J Radiol 85: 2288-2294, 2016.
47. Samiei S, van Nijnatten TJA, van Beek HC, Polak MPJ, Maaskant-Braat AJG, Heuts EM, van Kuijk SMJ, Schipper RJ, Lobbes MBI and Smidt ML: Diagnostic performance of axillary ultrasound and standard breast MRI for differentiation between limited and advanced axillary nodal disease in clinically node-positive breast cancer patients. Sci Rep 9: 17476, 2019.